


Nonergodic extended states in the β ensemble

Adway Kumar Das^{*} and Anandamohan Ghosh[†]

Department of Physical Sciences, Indian Institute of Science Education and Research Kolkata, Mohanpur, 741246 India

 (Received 3 January 2022; accepted 11 April 2022; published 12 May 2022)

Matrix models showing a chaotic-integrable transition in the spectral statistics are important for understanding many-body localization (MBL) in physical systems. One such example is the β ensemble, known for its structural simplicity. However, eigenvector properties of the β ensemble remain largely unexplored, despite energy level correlations being thoroughly studied. In this work we numerically study the eigenvector properties of the β ensemble and find that the Anderson transition occurs at $\gamma = 1$ and ergodicity breaks down at $\gamma = 0$ if we express the repulsion parameter as $\beta = N^{-\gamma}$. Thus other than the Rosenzweig-Porter ensemble (RPE), the β ensemble is another example where nonergodic extended (NEE) states are observed over a finite interval of parameter values ($0 < \gamma < 1$). We find that the chaotic-integrable transition coincides with the breaking of ergodicity in the β ensemble but with the localization transition in the RPE or the 1D disordered spin-1/2 Heisenberg model. As a result, the dynamical timescales in the NEE regime of the β ensemble behave differently than the latter models.

DOI: [10.1103/PhysRevE.105.054121](https://doi.org/10.1103/PhysRevE.105.054121)

I. INTRODUCTION

Canonically invariant classical ensembles including Dyson's threefold ways [1] and their extensions over symmetric spaces [2,3] (e.g., Laguerre [4], Jacobi [5], or circular [6] ensembles) are central to the paradigm of random matrix theory [7] epitomizing completely ergodic [8] and chaotic [9] dynamics in quantum mechanical systems. Corresponding energy levels tend to repel each other, where the degree of repulsion is called the Dyson's index, β , having values 1, 2, and 4 for the Gaussian orthogonal, unitary, and symplectic ensembles, respectively [10]. On the other hand, regular dynamics observed in integrable systems [11,12] is usually captured by the Poisson ensemble [13], where energy levels are uncorrelated with inclination to be clustered (and hence can be assigned $\beta = 0$). However, several physical systems (e.g., kicked top [14], pseudo-integrable billiards [15], Harper [16], Anderson model [17], etc.) show a spectral property intermediate between the aforementioned ideal limits. While phenomenological models [18–20] can mimic the spectral properties in the intermediate regions, there exist several generalizations of the classical ensembles capturing the physics of mixed dynamics [21–29]. In particular, the joint probability distribution function (JPDF) of eigenvalues for the classical ensembles can be expressed as a Gibbs-Boltzmann weight of a 2D system of particles, known as the Coulomb gas model [30], where β is no longer restrained to be quantized. Specifically, a harmonic confining potential yields the Gaussian β ensemble characterized by the following

JPDF:

$$P(\vec{E}) = \frac{1}{\mathcal{Z}_\beta} \exp\left(-\sum_{i=1}^N \frac{E_i^2}{2}\right) \prod_{i<j} |E_i - E_j|^\beta, \quad (1)$$

where \mathcal{Z}_β is the normalization constant and $\vec{E} = \{E_1, E_2, \dots, E_N\}$ is the set of N eigenvalues [31]. Such ensembles were originally conceived as lattice gas systems [32] in connection to the ground-state wave functions of the Calogero-Sutherland model [33]. Using $E_i \rightarrow \sqrt{\beta N} E_i$, we can express the partition function \mathcal{Z}_β as [34]

$$\mathcal{Z}_\beta \propto \int_{\mathbb{R}^N} \prod_{j=1}^N dE_j \exp(-\beta N^2 \mathcal{V}[\vec{E}]),$$

$$\mathcal{V}[\vec{E}] = \sum_{i=1}^N \frac{E_i^2}{2N} - \sum_{i \neq j} \frac{\ln |E_i - E_j|}{2N^2}, \quad (2)$$

where the potential $\mathcal{V}[\vec{E}]$ has a confining term competing with the pairwise logarithmic repulsion among N fictitious particles. The strength of such interactions is controlled by β [35], which can be interpreted as the inverse temperature of the Coulomb gas. In the infinite temperature limit ($\beta \rightarrow 0$), the energy levels are allowed to come arbitrarily close to each other, resulting in Poisson statistics, i.e., a signature of integrability [13]. On the other hand, for $\beta = 1$, Eq. (1) coincides with the JPDF of the Gaussian orthogonal ensemble (GOE), yielding Wigner-Dyson statistics characterized by complete level repulsion, i.e., a signature of chaos [9]. Thus tuning β , it is possible to control the degree of level repulsion in the energy spectrum of the β ensemble with $\beta = 1$ indicating the chaotic-integrable transition. Corresponding Hamiltonians can be represented as real, symmetric, and tridiagonal $N \times N$

^{*}akd19rs062@iiserkol.ac.in

[†]anandamohan@iiserkol.ac.in

matrices, H , with following nonzero elements [36]:

$$\begin{aligned} H_{i,i} &= A_i, \quad H_{i,i+1} = H_{i+1,i} = B_i/\sqrt{2}, \\ A_i &\sim \mathcal{N}(0, 1), \quad B_i \sim \chi_{(N-i)\beta}, \end{aligned} \quad (3)$$

where $\mathcal{N}(0, 1)$ is the Normal distribution and χ_k is the chi distribution with a degree of freedom k . There have been extensive studies on β ensemble in terms of the density of states (DOS) [32,37–39], associated fluctuations [40–44], connection to stochastic differential operators [45–47], and extreme eigenvalues [48–51]. In this work we give numerical evidence of chaotic \rightarrow integrable, ergodic \rightarrow nonergodic, and delocalization \rightarrow localization transitions by thoroughly studying the properties of eigenvalues (Sec. II), eigenfunctions (Sec. III), and dynamics (Sec. IV). Therefore we identify the critical values of β segregating ergodic, nonergodic extended (NEE), and localized regimes. We compare the spectral properties of the β ensemble with the properties of another matrix model, namely Rosenzweig-Porter ensemble (RPE) [21,52], where for a real symmetric matrix, H , all the elements are randomly distributed with

$$H_{i,i} \sim \mathcal{N}(0, 1), \quad H_{i,j}/\sigma \sim \mathcal{N}(0, 1), \quad \sigma^2 = 1/2N^{\tilde{\gamma}}, \quad \tilde{\gamma} \in \mathbb{R}. \quad (4)$$

Moreover, as an impetus to applications in physical systems, we compare both the β ensemble and RPE to the widely studied 1D disordered spin-1/2 Heisenberg model [53–55], where for simplicity we will consider the chain to be isotropic. The Hamiltonian of such a chain of length L with magnetic field in the Z direction is defined as

$$H = -\frac{J}{2} \sum_{i=1}^L \bar{\sigma}_i \cdot \bar{\sigma}_{i+1} + h_i \hat{\sigma}_i^z, \quad (5)$$

where $\bar{\sigma}_i = \{\hat{\sigma}_i^x, \hat{\sigma}_i^y, \hat{\sigma}_i^z\}$ are the Pauli matrices, h_i is the random magnetic field applied in the Z direction on the i th site, and J is the coupling constant. We assume a periodic boundary condition (i.e., $\hat{\sigma}_{i+L}^\alpha = \hat{\sigma}_i^\alpha$), $J = 1$, and h_i to be uniform random numbers sampled from $[-h, h]$, so the disorder in Heisenberg model can be controlled by tuning h . While the model is integrable exactly at $h = 0$, even an infinitesimal fluctuation in magnetic fields on different sites is expected to induce chaos in the thermodynamic limit ($L \rightarrow \infty$) [54]. Increasing h further introduces more defects in the chain leading to many-body localization (MBL) where the critical disorder strength, h_c for the ergodic to MBL transition depends on the energy density [55]. Since the Z component of total spin, $S_z = \frac{1}{2} \sum_{i=1}^L \hat{\sigma}_i^z$, is conserved in the Heisenberg model, we take L to be even and choose the largest symmetry sector $S_z = 0$ having $\binom{L}{L/2}$ eigenvalues for our analysis.

One can intuitively speculate the existence of two critical points in the β ensemble, considering that the diagonal part, A , is competing with the perturbation from the off-diagonal part B . The overall interaction strength can be calculated in terms of the Frobenius norm of B , i.e., $\|B\|_F \approx \sqrt{\sum_{i=1}^{N-1} B_i^2} = \sqrt{\frac{1}{2}N(N-1)\beta} \approx N\sqrt{\beta}$, where $\bar{B}_i^2 = (N-i)\beta$ is the mean value of B_i^2 (as the χ_k^2 distribution has mean k). Similarly, the strength of the diagonal contribution is $\|A\|_F \approx \sqrt{N}$. Thus for the weak perturbation ($\|B\|_F < \|A\|_F \Rightarrow \beta < 1/N$), one may expect the energy states of the β ensemble to localize,

while they should be extended for $\|B\|_F > \|A\|_F$. Therefore it is convenient to express the Dyson's index as

$$\beta = N^{-\gamma}, \quad \gamma \in \mathbb{R}. \quad (6)$$

So the perturbation strength can be expressed as $\|B\|_F = N^{1-\gamma/2}$, and it is reasonable to expect that $\gamma_{AT} \equiv 1$ is the Anderson transition point such that the energy states are localized for $\gamma > \gamma_{AT}$.

The role of the control parameter manifested in the off-diagonal terms of the β ensemble is reminiscent of the RPE, where relative strength of perturbation indicates that Anderson transition occurs at $\tilde{\gamma}_{AT} = 2$ [56]. Moreover, due to the random sign altering nature of the RPE matrix elements, there exists an ergodic transition at $\tilde{\gamma}_{ET} = 1$ segregating three distinct phases: ergodic, NEE, and localized states [56]. Similarly, for the β ensemble, even though the off-diagonal elements, B_i , are strictly positive, the diagonal terms, A_j , can be positive or negative at random. If we equate the rescaled perturbation, $\|B\|_F/\sqrt{N}$ to the total fluctuation from on-site terms, $\|A\|_F$, we expect ergodic transition at $\gamma_{ET} \equiv 0$ such that the energy states occupy the entire Hilbert space in the regime $\gamma \leq \gamma_{ET}$. However, these heuristic arguments based on the norm alone cannot account for any phase transition. For example, eigenvectors are exponentially localized in tridiagonal matrices with i.i.d. random elements [57]. Thus the inhomogeneity of the off-diagonal terms evident from Eq. (3) is essential for the existence of NEE in the β ensemble as will be demonstrated in the following sections.

II. PROPERTIES OF ENERGY LEVELS

Now we would like to study the energy level properties of the β ensemble following the Hamiltonian in Eq. (3) and identify the transition from integrable to chaotic regimes as we vary the Dyson's index. We also compare the properties of the β ensemble with the results known for RPE and Heisenberg model. Some of the results in this section are known, and we list them for completeness.

A. Density of states (DOS)

As a starting point, we look at the DOS, which is the marginal PDF of energy levels. The bulk eigenvalues of the β ensemble roughly scale with system size as $\epsilon_\beta = \sqrt{4 + 2N^{1-\gamma}}$ [58]. So we scale the eigenvalues as $E \rightarrow E/\epsilon_\beta$ and obtain the DOS numerically, as shown in Fig. 1(a) for $N = 8192$ and various γ . For $\gamma > 1$ we obtain $\epsilon_\beta \approx 2$ such that the DOS converges to the Gaussian distribution, $\mathcal{N}(0, 1/4)$ with increasing N , as illustrated in Fig. 1(c) for a specific value of $\gamma = 1.1$. Exactly at $\gamma = 1$, the DOS is system size independent and follows a shape intermediate between Gaussian distribution and Wigner semicircle law since $\epsilon_\beta = \sqrt{6}$. But for $0 \leq \gamma < 1$, the DOS converges to the semicircle law upon increasing N , as shown in Fig. 1(b) for a specific value of $\gamma = 0.6$. However, in the limit $\beta \rightarrow \infty$ (i.e., $\gamma < 0$ and $N \rightarrow \infty$), all the eigenvalues of the β ensemble freeze and produce a picket-fence spectrum [59]. A qualitative evolution of the shape of the DOS in the β - N plane is shown in Fig. 2 of reference [35].

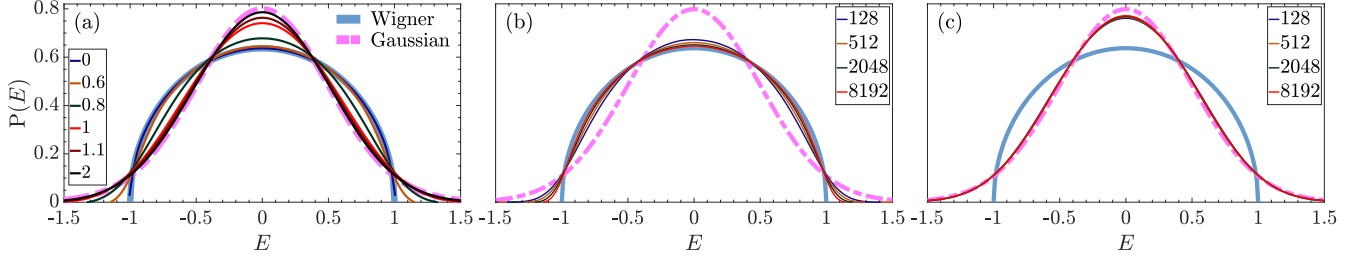


FIG. 1. Density of states (DOS) of the β ensemble (a) averaged over 500 disordered realizations for various γ where $N = 8192$. (b) $\gamma = 0.6$ and (c) $\gamma = 1.1$ for various N . We also show Wigner's semicircle law (solid bold) and Gaussian distribution $\mathcal{N}(0, 1/4)$ (dashed bold).

In case of the RPE, bulk eigenvalues scale as $\epsilon_{\text{RPE}} = \sqrt{4 + 2N/\sigma^2} = 2\sqrt{1 + N^{1-\tilde{\gamma}}}$. Consequently the scaled DOS of RPE ($E \rightarrow E/\epsilon_{\text{RPE}}$) varies from Wigner's semicircle to a Gaussian similar to the β ensemble as $\tilde{\gamma}$ is increased from 0. Contrarily for 1D disordered spin-1/2 Heisenberg model, DOS always follows a Gaussian distribution spreading with the disorder strength, which is typical of many-body systems with local interactions [60]. However, the differences in global shapes of DOS from these different models do not dictate the correlations in the respective local energy scales as demonstrated below.

B. Nearest-neighbor spacing (NNS)

One of the most commonly investigated quantity reflecting local spectral correlations is the distribution of nearest-neighbor spacing (NNS) of the ordered and unfolded eigenvalues (see the Appendix), which follows Wigner's surmise and exponential distribution for the chaotic and integrable systems, respectively [7]. As the nature of correlation present in the spectrum edge is different than that of the bulk energy levels, we numerically evaluate the PDF of NNS

choosing only the middle 25% of the spectrum. The results for $N = 8192$ are shown in Fig. 2(a) with markers along with the approximate empirical PDF of NNS [Eqs. (12) and (13) in [35]], which is N -independent, provided $N \gg 1$. Such a functional form also implies that for $s \ll 1$, $P(\beta; s) \sim s^\beta \forall \beta$, thus the degree of level repulsion is indeed quantified via β , as expected from Eq. (1). We observe a crossover from Wigner's surmise to exponential distribution in Fig. 2(a) as we decrease β , implying a suppression of chaos. A similar crossover is observed in RPE [61] and 1D disordered spin-1/2 Heisenberg model [61] as well.

C. Ratio of nearest-neighbor spacing (RNNS)

Another notable measure of the short-range spectral correlations is the ratio of nearest-neighbor spacing (RNNS), which is much simpler to study since unfolding of the energy spectrum is not required [63,64]. If we define $\tilde{r}_i = \min\{r_i, 1/r_i\}$, where r_i is the i th RNNS, then $P(\tilde{r}) = 2P(r)\Theta(1-r)$, with $\Theta(x)$ being the Heaviside step function. We show the PDF of \tilde{r} with markers in Fig. 2(b) for $N = 8192$ along with the empirical PDF of RNNS [Eq. (1) in [65]]. Again a crossover

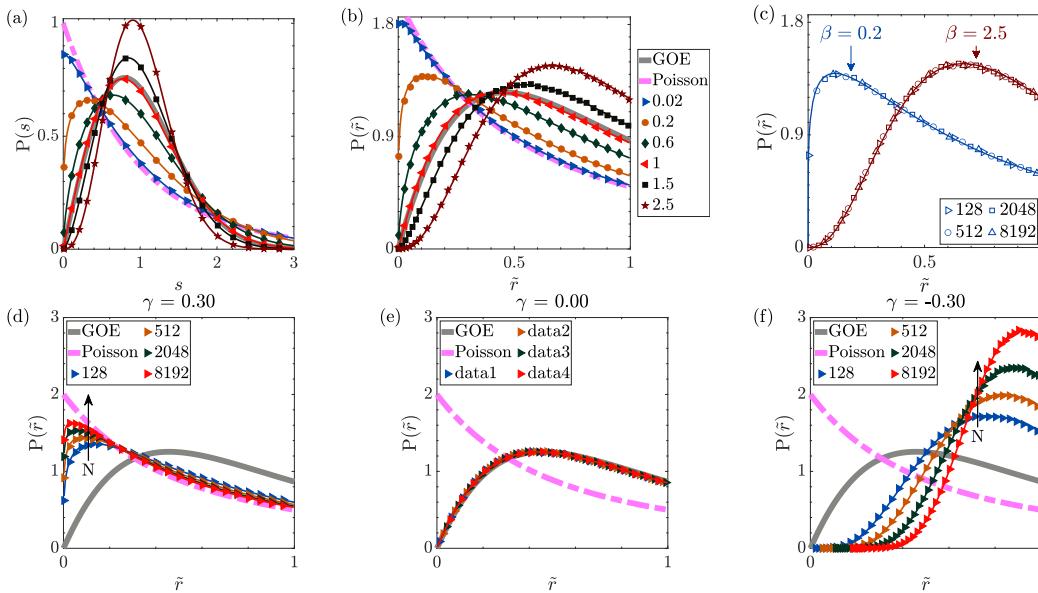


FIG. 2. Short-range spectral correlations for β ensemble: PDF of (a) NNS and (b) modified RNNS varying β for $N = 8192$, and varying N for $\beta = 0.2$ and 2.5 (c), $\gamma = 0.3$ (d), $\gamma = 0$ (e), and $\gamma = -0.3$ (f). The markers indicate numerical data, while solid lines denote empirical analytical forms [Eqs. (12) and (13) in [35] for NNS and Eq. (1) in [65] for RNNS]. We also show analytical expressions for the Poisson ensemble (dashed bold) and GOE (solid bold).

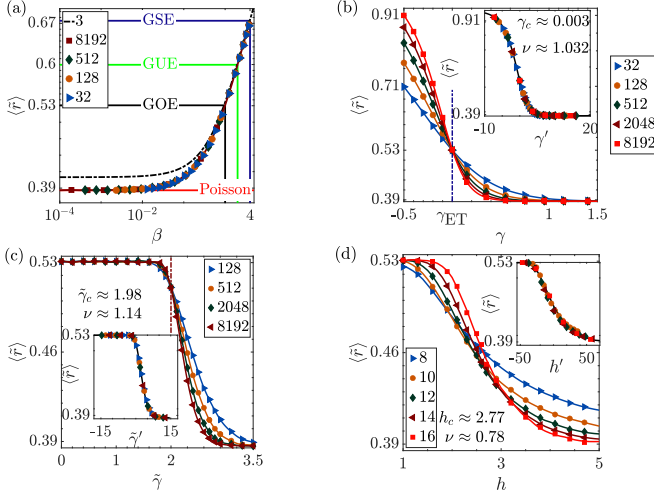


FIG. 3. Ensemble average of \tilde{r} for β ensemble vs (a) β and (b) γ , and (c) for RPE vs $\tilde{\gamma}$ and (d) Heisenberg model vs disorder strength, h . For (a), (b), and (c) system size, N , and for (d) chain length, L , is varied. In (a) we show the $\langle \tilde{r} \rangle$ for $N = 3$ [Eq. (7) in [63]] with a dashed line. The insets of (b), (c), and (d) show collapsed data following the ansatz in Eq. (7), where critical parameter and exponents are also given.

w.r.t. β is immediately apparent. For $N \gg 1$, the density of RNNS is system size independent, as shown in Fig. 2(c) for two values of β while varying N . This can be inferred from Fig. 3(a) as well, where the ensemble-averaged values of \tilde{r} as a function of β collapse for different N provided $N \gg 1$. In Figs. 2(d), 2(e), and 2(f), we show the density of \tilde{r} for different values of γ while varying N . For any value of $\gamma < 0$ as $N \rightarrow \infty$ (i.e., $\beta \rightarrow \infty$), the energy levels are highly correlated and strongly repel each other. The increase in level repulsion with N is shown in Fig. 2(f) for a fixed value of $\gamma = -0.3$. Exactly at $\gamma = 0$ (i.e., $\beta = 1$) the density of \tilde{r} is independent of N and matches that of the GOE [Fig. 2(e)]. On the other hand, for any $\gamma > 0$ and $N \rightarrow \infty$ (i.e., $\beta \rightarrow 0$), the energy levels become uncorrelated and clustered as in the Poisson ensemble. In Fig. 2(d) we show that the density of \tilde{r} converges towards Poisson expression as we increase N for a fixed value of $\gamma = 0.3$. These analyses imply that the signatures of chaos in the short-range spectral correlations are lost as we lower the repulsion parameter β . Now we identify the exact nature of such a transition.

D. Criticality in chaotic-integrable transition

For a fixed γ , the quick convergence of PDF of RNNS with system size [Fig. 3(a)] enables us to conclude that the $\langle \tilde{r} \rangle$ has one-to-one correspondence with β when $N \gg 1$. β increases with N for any $\gamma < 0$ (as $\beta = N^{-\gamma}$), hence $\langle \tilde{r} \rangle$ should also increase with N and vice versa. Figure 3(b) conforms to the above expectations suggesting a scaling hypothesis for $\langle \tilde{r} \rangle$. Let us assume that there exists a relevant correlation length Ξ showing a power-law divergence around a critical point, γ_c , i.e., $\Xi \sim (\gamma - \gamma_c)^{-\nu}$, where ν is a critical exponent. Then any quantity $A(\gamma, N)$ showing nonanalytical behavior close to γ_c

should behave as

$$A(\gamma, N) \propto f((\gamma - \gamma_c)(\ln N)^{1/\nu}), \quad (7)$$

where f is a universal function and we assume Ξ to scale with $\ln N$ instead of N . Such a scaling ansatz valid for a second-order phase transition is shown to hold in case of the Kullback-Leibler divergence of RPE [61]. We collapse the crossover curves from different system sizes based on Eq. (7) (see the Appendix) and obtain $\gamma_c = 0.0030$ and $\nu = 1.0316$ as shown in the inset of Fig. 3(b). Such a critical behavior can also be inferred from the scale invariance of $\langle \tilde{r} \rangle$ w.r.t. $-\ln \beta = \gamma \ln N$ [Fig. 3(a)]. Comparing this with Eq. (7), we get $\gamma_c = 0$ and $\nu = 1$, which is consistent with our numerical analysis.

We show the $\langle \tilde{r} \rangle$ curves for different system sizes and chain lengths in Figs. 3(c) and 3(d) for RPE and Heisenberg model, respectively. Again assuming a power-law behavior like Eq. (7), we are able to collapse the data for RPE using $\tilde{\gamma}_c \approx 1.9750$, $\nu \approx 1.1359$. For the Heisenberg chain we assume that $A(\gamma, N) \propto f((h - h_c)L^{1/\nu})$ and get $h_c \approx 2.7696$, $\nu \approx 0.7842$. Note that the critical disorder strength found here corresponds to the middle 25% of the eigenspectrum and hence conforms to the energy density phase diagram of MBL transition present in the literature [55].

Thus we show that the chaotic-integrable transition in all three models is second order in nature. The crucial difference lies in the physical significance of these critical points. We observe that the chaotic-integrable transition occurs at $\tilde{\gamma}_{AT}$ in the case of RPE, i.e., the energy states localize as soon as the energy levels start to cluster. Contrarily in the case of the β ensemble, a chaotic-integrable transition occurs at $\gamma = 0$, which we previously argued to be γ_{ET} , i.e., where ergodicity breaks down. Thus in the thermodynamic limit ($N \rightarrow \infty$), there will be extended states for which energy levels are uncorrelated, which has a profound implication on the dynamical properties of the β ensemble (see Sec. IV). Thus our analysis shows that the eigenstate localization property is not necessarily indicative of the degree of repulsion present in the energy spectrum as also observed in certain structured matrix ensembles [66–68].

E. Power spectrum

Short-range spectral correlations in the β ensemble exhibit criticality only around $\gamma_{ET} = 0$. We also expect a second critical point associated with the localization transition, which can be captured by the long-range spectral correlations, e.g., the power spectrum of δ_n statistics [69,70],

$$P_k^\delta = |\hat{\delta}_k|^2, \quad \hat{\delta}_k = \frac{1}{\sqrt{N}} \sum_n \delta_n \exp\left(-\frac{i2\pi kn}{N}\right), \quad (8)$$

where $\delta_n \equiv \mathcal{E}_n - n$ is the fluctuation of the n th unfolded energy level, \mathcal{E}_n , around its mean value, n . The ensemble average of P_k^δ , denoted by $\langle P_k^\delta \rangle$, is explored for the 1D disordered spin-1/2 Heisenberg model in [71,72]. In the β ensemble, there exists a critical frequency $k_c = N^{1-\gamma}/2$ for $\gamma \geq 0$ [73] such that for $k \leq k_c$, $\langle P_k^\delta \rangle \propto 1/k$ identifying completely chaotic behavior whereas for $k > k_c$, $\langle P_k^\delta \rangle \propto 1/k^2$, which is a signature of the Poisson ensemble. Note

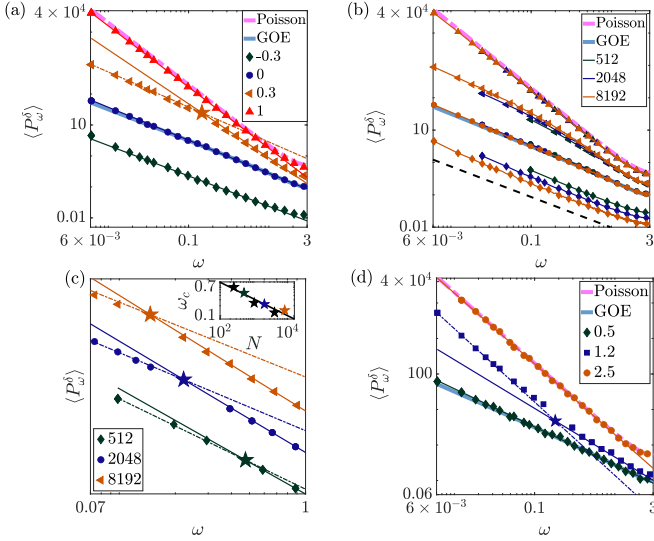


FIG. 4. Power spectrum of noise for (a) the β ensemble and (d) RPE for $N = 8192$ as a function of dimensionless frequency, $\omega = 2\pi k/N$. In (b), the power spectrum is shown for various γ [denoted with markers similar to (a)] and N (denoted by different colors as in the legend). We see that $\langle P_\omega^\delta \rangle$ shifts downwards with increasing N for $\gamma = -0.3$, where the dashed line $\propto 1/\omega$ is placed as a guide to the eye. (b) $\langle P_\omega^\delta \rangle$ for $\gamma = 0.3$ while varying N (data shifted in the Y direction for clarity). Dashed and solid lines indicate $1/\omega$ and $1/\omega^2$ behaviors, respectively. In (a), (c), and (d), stars denote the critical frequencies, ω_c , separating heterogeneous behavior. The inset of (c) shows numerically obtained ω_c , where the solid line denotes the linear fit in log-log scale. We also show the analytical $\langle P_\omega^\delta \rangle$ for the Poisson ensemble (dashed bold) and GOE [solid bold; Eq. (10) in [69]].

that the power spectrum of some physical systems like the Robnik billiard [74] and kicked top [75] exhibit a homogeneous behavior, $\langle P_k^\delta \rangle \propto 1/k^\alpha$, across all frequencies with $1 < \alpha < 2$.

In Fig. 4(a), we show the power spectrum of the β ensemble as a function of dimensionless frequency, $\omega = 2\pi k/N$, for $N = 8192$ and various γ with the bold curves showing the analytical forms of $\langle P_\omega^\delta \rangle$ for the Poisson ensemble and GOE [Eq. (10) in [69]]. In Fig. 4(b) we show $\langle P_\omega^\delta \rangle$ for same values of γ but also by varying N denoted with different colors. We see that for finite N and $\gamma < 0$, $\langle P_\omega^\delta \rangle \propto 1/\omega$ for a typical value of $\gamma = -0.3$. However, we observe that for $N \gg 1$ and $\gamma \ll 0$ (i.e., $\beta \rightarrow \infty$), there are fluctuations around $1/\omega$ behavior due to the energy spectrum attaining a picket-fence structure. For $\gamma \geq 0$, we can identify two critical points separating three distinct regimes by looking at Fig. 4(b) or from the analytical calculations in [73]:

(a) $\gamma = 0$: $\langle P_\omega^\delta \rangle \propto 1/\omega$ for any $N \Rightarrow$ energy levels are correlated at all scales even in the thermodynamic limit

(b) $0 < \gamma < 1$: Heterogeneous spectra $\Rightarrow \omega_c = 2\pi k_c/N = \pi N^{-\gamma}$ separating the Poisson ensemble and GOE like scaling. In Fig. 4(c) we show $\langle P_\omega^\delta \rangle$ for $\gamma = 0.3$ and various N , which clearly reflects the heterogeneous features. In the inset we show numerically obtained ω_c vs N .

(c) $\gamma \geq 1$: $\langle P_\omega^\delta \rangle \propto 1/\omega^2$ for any $N \Rightarrow$ energy levels are uncorrelated at all scales even in the thermodynamic limit.

Note that $k_c \rightarrow \infty$ for $N \rightarrow \infty$ and $0 < \gamma < 1$, i.e., the signature of chaotic spectrum prevails over infinitely many frequencies. However, their support set constitutes a zero fraction of the set of principal frequencies as $k_c/k_{\text{Nyquist}} = N^{-\gamma} \rightarrow 0$ for any $\gamma > 0$ ($k_{\text{Nyquist}} \approx N/2$ is the highest frequency required to fully reconstruct the original spectrum [69]). Such a fractal behavior suggests the absence of ergodicity in the β ensemble for $0 < \gamma < 1$. For example, in the case of RPE, eigenstates occupy a zero fraction of the Hilbert space volume despite being extended in the NEE phase ($1 \leq \tilde{\gamma} < 2$) [56]. A corresponding power spectrum also exhibits heterogeneous behavior as shown in Fig. 4(d). Thus we can attribute the heterogeneity in the power spectrum of δ_n statistics to the existence of NEE phase, and we can conclude that the β ensemble enters the NEE phase for $0 < \gamma < 1$ where ergodicity breaks down at $\gamma_{\text{ET}} = 0$ and the Anderson transition occurs at $\gamma_{\text{AT}} = 1$.

With this primary evidence of the existence of the NEE regime in the β ensemble, in the next section we will study the eigenfunction properties and obtain the fractal scaling of NEE states.

III. PROPERTIES OF EIGENSTATES

Due to the canonical invariance, the eigenvectors of $N \times N$ GOE matrices are uniformly distributed in the unit N -dimensional sphere, resulting in mutually independent eigenvector components. Contrarily for the β ensemble, all elements but the first component of the k th eigenvector can be expressed in terms of the k th eigenvalue and different matrix elements [36]. Hence even for typical values of β (i.e., $\beta = 1, 2, 4$), the eigenvector properties of the Wigner-Dyson and β ensembles are different from each other, although their energy level statistics are identical. This can be readily verified from the distribution of $\ln(N|\Psi_i|^2)$ (Ψ_i is i th component of the eigenstate $|\Psi\rangle$), which has a long tail for $\beta = 1$ in the β ensemble compared to GOE.

A. Localization transition

In order to characterize the Anderson transition from the properties of eigenstates, we begin by computing the Shannon entropy, defined as $S = -\sum_{i=1}^N P_i \ln(P_i)$ with $P_i = |\Psi_i|^2$. In Fig. 5(a) we show ensemble-averaged S , obtained from the eigenstates taken from the middle 25% of the spectra, exhibiting a nonanalyticity around $\gamma = 1$. Assuming a power-law behavior of the relevant correlation length, we obtain the critical parameter $\gamma_c = 0.95$ and exponent $\nu = 0.65$ using Eq. (7), while the collapsed data are shown in the inset of Fig. 5(a). We also observe that the inverse participation ratio (IPR), $I = \sum_{i=1}^N |\Psi_i|^4$, exhibits a criticality around $\gamma = 1$ as shown in Fig. 6. Thus we confirm that the Anderson transition occurs at $\gamma_{\text{AT}} \equiv 1$ for the β ensemble, and at $\tilde{\gamma}_{\text{AT}} \simeq 2$ for RPE [Fig. 5(b)].

For the 1D disordered spin-1/2 Heisenberg model, Shannon entropy is almost constant for a particular L if the disorder strength is small ($h \ll 1$) and slowly decaying for $h \gg 1$. Similar behavior for IPR indicates that the energy states of the Heisenberg model in the MBL regime are extended in the Hilbert space exhibiting a nontrivial multifractal behavior [55]. However, according to [54], one may look at the ratio

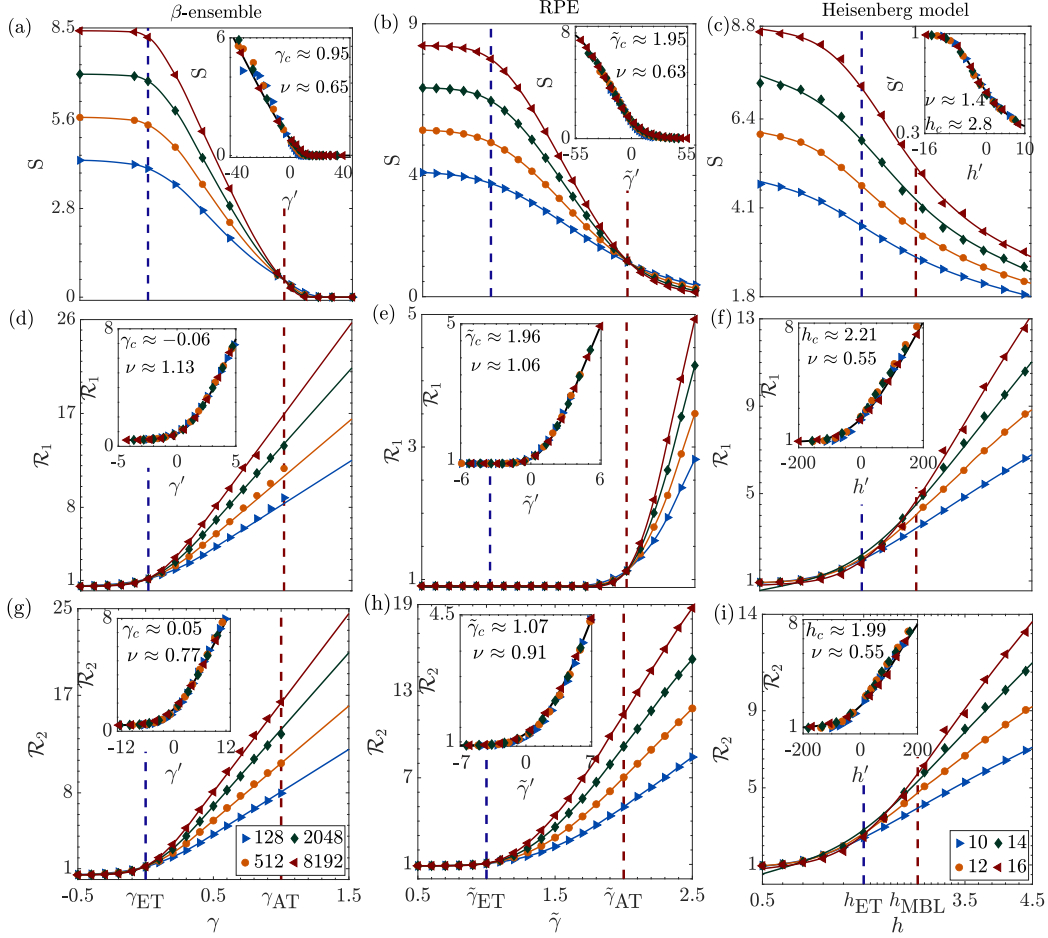


FIG. 5. Eigenstate statistics: Shannon entropy, S , and relative Rényi entropy of two types [$\mathcal{R}_{1,2}$ in Eq. (9)] for the β ensemble, RPE, and 1D disordered spin-1/2 Heisenberg model, as a function of system parameters for different matrix size, N , and chain length, L (values given in the legends). The critical values of parameters indicating ergodic and localization transitions are marked with a dashed line in all plots. The inset shows collapsed data following the ansatz in Eq. (7), where numerically obtained critical parameters and exponents are also given. The inset of (c) shows collapsed data of $S' = S/\ln(0.48N)$.

of Shannon entropies of the Heisenberg model and GOE, i.e., $S' = S/S_{\text{GOE}} \approx S/\ln(0.48N)$, where $N = \binom{L}{L/2}$ is the Hilbert space dimension of the $S_z = 0$ symmetry sector. The finite-size scaling of S' gives the numerical estimate of the MBL transition point to be $h_{\text{MBL}} \approx 2.77$ for our choice of $L = 8, 10, \dots, 16$. This is the same critical point beyond which energy levels start to cluster [Fig. 3(d)]. Such a conclusion is also

verified via studies of entanglement entropy and magnetization fluctuations [55]. Thus unlike the β ensemble, eigenstates start to localize as soon as energy levels begin to cluster for both the RPE and 1D disordered spin-1/2 Heisenberg model.

B. Ergodic to nonergodic transition

We now quantify the loss of ergodicity by computing the relative Rényi (\mathcal{R}) entropy between a pair of eigenfunctions [76] having similar energy densities. Let $|\Psi_i^j\rangle$ be the i th eigenvector of the j th disordered realization of an ensemble. We define two kinds of \mathcal{R} as follows:

$$\mathcal{R}_1 = -2 \ln \left(\sum_{k=1}^N |\Psi_i^j(k) \Psi_{i+1}^j(k)| \right),$$

$$\mathcal{R}_2 = -2 \ln \left(\sum_{k=1}^N |\Psi_i^j(k) \Psi_{i+1}^{j'}(k)| \right). \quad (9)$$

Here \mathcal{R}_1 and \mathcal{R}_2 measure similarity among wave functions obtained from the same and different samples, respec-

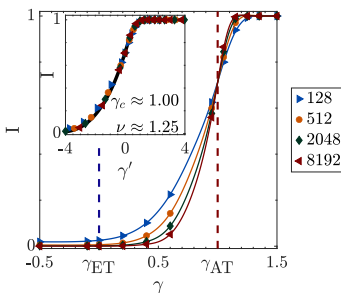


FIG. 6. Inverse participation ratio: for β ensemble as a function of γ for various system sizes, N . Inset shows collapsed data following the ansatz in Eq. (7) along with critical parameter and exponent.

tively. For eigenstates of GOE, $\mathcal{R} = -2 \ln(\sum_{k=1}^N |z_k|)$, $z_k = x_k \times y_k$, where x_k, y_k are i.i.d. random variables and for $N \gg 1$, $x_k, y_k \sim \mathcal{N}(0, 1/\sqrt{N}) \forall k$ assuming wave functions are normalized. Then $P(z) = NK_0(N|z|)/\pi$, where $K_0(x)$ is the modified Bessel function of the second kind. Then $\langle |z| \rangle = 2/N\pi$ and

$$\langle \mathcal{R} \rangle = -2 \ln \left(\sum_{i=1}^N \frac{2}{N\pi} \right) = 2 \ln \left(\frac{\pi}{2} \right) \approx 0.9. \quad (10)$$

Thus $\mathcal{R} \approx 0.9$ for any pair of completely extended wave functions, and this value is used to benchmark our numerical estimates. The relative Rényi entropy can be viewed as a generalization of the Kullback-Leibler divergence exhibiting critical behavior in the case of RPE [61]. We will investigate \mathcal{R}_1 and \mathcal{R}_2 in the similar spirit with the premise of finding the following:

(a) Ergodic regime: $\mathcal{R} \sim O(1)$ for any pair of wave functions, as both of them are uniformly extended

(b) Localized regime: \mathcal{R} will diverge as different wave functions localized at separate sites

(c) Nonergodic regime having two possibilities:

(1) If energy levels of $|\Psi_i^j\rangle, |\Psi_{i'}^j\rangle$ repel each other, then such energy states come from the same symmetry sector, i.e., the same subspace of the Hilbert space. Thus $|\Psi_i^j\rangle, |\Psi_{i'}^j\rangle$ are likely to hybridize if the governing Hamiltonian is sufficiently dense [61], giving $\mathcal{R} \sim O(1)$.

(2) In the absence of any level repulsion, the energy states in the NEE phase are likely to be extended over different parts of the Hilbert space, thus \mathcal{R} will diverge.

Let us now illustrate the measures for the well-studied case of RPE. For two nearby energy states $|\Psi_i^j\rangle, |\Psi_{i'}^j\rangle$ with comparable energy densities, $\mathcal{R}_1 \sim O(1)$ for $\tilde{\gamma} < \tilde{\gamma}_{AT}$ and $\mathcal{R}_1 \gg 1$ for $\tilde{\gamma} > \tilde{\gamma}_{AT}$ as a chaotic-integrable transition occurs at $\tilde{\gamma}_{AT}$. On the other hand, the energy states from different samples, say, $|\Psi_i^j\rangle, |\Psi_{i'}^{j'}\rangle$, are likely to have a different support set in the NEE phase, as different governing Hamiltonians cannot hybridize them even if their energy densities are comparable, giving $\mathcal{R}_2 \gg 1$ for $\tilde{\gamma} > \tilde{\gamma}_{ET}$. In Figs. 5(e) and 5(h) we show $\mathcal{R}_1, \mathcal{R}_2$ for RPE exhibiting second-order phase transitions clearly identifying the critical points $\tilde{\gamma}_{AT}$ and $\tilde{\gamma}_{ET}$, respectively.

Recall that for the β ensemble chaotic-integrable transition occurs at $\gamma_{ET} = 0$, hence \mathcal{R}_1 should show nonanalyticity at the same point. Previously we argued that γ_{ET} is also the ergodic transition point, thus \mathcal{R}_2 should exhibit criticality there as well. The critical behaviors of $\mathcal{R}_1, \mathcal{R}_2$ are evident in Figs. 5(d) and 5(g), where scaling analysis gives $\gamma_c \equiv \gamma_{ET} \sim 0$.

In the case of the 1D disordered spin-1/2 Heisenberg model, we find that the scaling of \mathcal{R}_2 indicates a $h_c \equiv h_{ET} \approx 2$ in Fig. 5(i), while earlier we identified $h_{MBL} \approx 2.77$. This indicates the existence of NEE in the 1D disordered spin-1/2 Heisenberg model for an intermediate range of disorder $h \in (2, 2.77)$ in agreement with the existing studies on participation entropy, survival probability [54], and momentum distribution fluctuations [71]. Therefore one would expect \mathcal{R}_1 to show criticality at h_{MBL} since it is also the chaotic-integrable transition point. However, the Hamiltonians of the

1D disordered spin-1/2 Heisenberg model are so sparse in that they fail to completely hybridize the NEE eigenstates even from the same subspace of the Hilbert space. As a result \mathcal{R}_1 shows criticality at $h_c \approx 2.21$ [Fig. 5(f)], a value in between h_{ET} and h_{MBL} . Below the critical values, $\mathcal{R} \approx 0.9$ in all three models as expected from Eq. (10).

C. Localization length

In the previous section, we noticed that the spectral properties of the β ensemble and RPE have an important difference: the chaotic-integrable transition occurs at γ_{ET} for the β ensemble and $\tilde{\gamma}_{AT}$ for RPE. The degree of level repulsion, β , has been interpreted as the rescaled localization length in various systems [77–80] though there are exceptions as well [81]. Now we look at the entropic localization length w.r.t. the Shannon entropy, $d_N \equiv 2.07e^S$, such that $d_N \approx N$ or $d_N \approx 1$ for a fully ergodic or localized energy state, respectively [77]. In the case of RPE or the 1D disordered spin-1/2 Heisenberg model, one can numerically fit the PDF of NNS with any phenomenological model (e.g., Brody [18], Berry-Robnik [19], etc.) to estimate the repulsion parameter, β . However, such a numerical fit pertains to the global shape of the PDF of NNS [77], without necessarily reflecting the behavior of $P(s)_{s \rightarrow 0}$, which is the true measure of level repulsion in a system. Thus we exploit the one-to-one correspondence between β and the mean value of RNNS. We observe a sublinear behavior when β is small and d_N/N converges to 1 when $\beta \rightarrow 1$ [Figs. 7(b) and 7(c)]. Hence energy states are completely extended whenever the energy levels repel each other, and this justifies the coincidence of chaotic-integrable transition with the delocalization-localization transition in RPE and the 1D disordered spin-1/2 Heisenberg model.

We show d_N/N as a function of β for various system sizes in the case of the β ensemble in Fig. 7(a). Here the relationship between the localization length and the degree of level repulsion is superlinear throughout. Moreover, d_N/N becomes independent of β for $\beta \leq \beta^* \ll 1$ while $\beta^* \propto 1/N$ as shown in the inset of Fig. 7(a). This implies that the localization transition should occur roughly at $\beta = 1/N$ as the chaotic-integrable transition occurs at $\beta = N^{\gamma_{ET}} = 1$. This supports our earlier observation that $\gamma_{AT} = 1$ does not coincide with the chaotic-integrable transition point in the case of the β ensemble unlike RPE or the Heisenberg model.

D. Scaling of eigenstate fluctuations

It is important to analyze the eigenfunction fluctuations, which can be quantified via Rényi entropy, $S_R(q, N) \sim N^{D_q}$, where D_q are fractal dimensions for different values of q [82]. For $q = 1$, the Rényi entropy converges to the Shannon entropy, $S \sim D_1 \ln N$. Similarly for $q = 2$, one obtains the scaling in IPR $\sim N^{-D_2}$. In the ergodic regime the fractal dimensions, $D_{1,2} = 1$, as eigenstates occupy the full Hilbert space volume, while $D_{1,2} = 0$ in the localized regime. In the NEE phase, $0 < D_{1,2} < 1$, which implies that the eigenstates are extended over infinitely many but a zero fraction of all possible sites in the thermodynamic limit (i.e., $N^{D_{1,2}} \rightarrow \infty$ but $N^{D_{1,2}}/N \rightarrow 0$ if $N \rightarrow \infty$). Since dis-

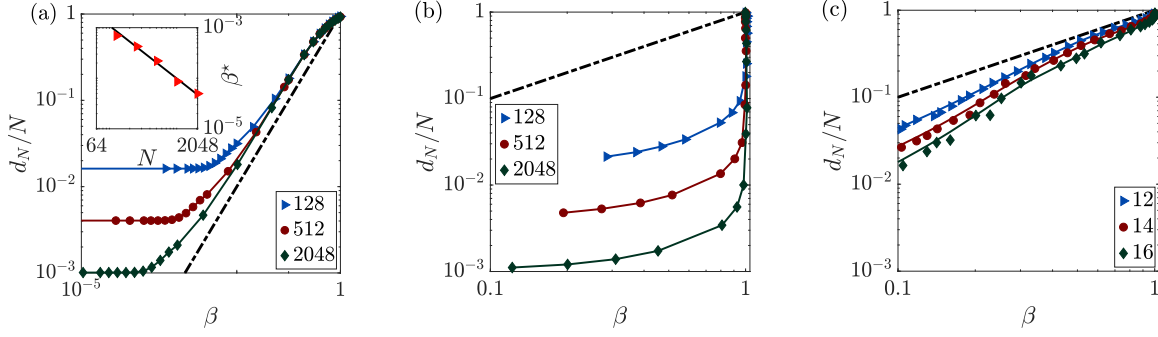


FIG. 7. Entropic localization length for (a) the β ensemble, (b) RPE, and (c) 1D disordered spin-1/2 Heisenberg model for various system sizes and chain lengths as a function of the repulsion parameter β . We show the line $d_N/N = \beta$ with a dashed curve. The inset of (a) shows β^* below which d_N/N becomes constant.

tributions of Shannon entropy and IPR are quite broad and skewed [Fig. 8(a)], the median instead of the mean has been used to estimate such fractal dimensions [83]. The numerically estimated $D_{1,2}$ clearly identifies the ergodic, NEE, and localized regimes for the β ensemble and RPE as shown in Fig. 9 ($D_{1,2} \approx 1 - \gamma$ and $2 - \tilde{\gamma}$ in the NEE phase for the β ensemble and RPE, respectively). However, for the Heisenberg model, $D_{1,2}$ does not vanish for $h > h_{\text{MBL}}$ resulting from nontrivial multifractality in the MBL phase [55].

To probe finer details of the eigenstructure of β ensemble, we look at the density of Shannon entropy. The distributions from different system sizes collapse on top of each other at $\gamma = 0, 1$ upon a rescaling $S \rightarrow S - D_1 \ln N$. However, in the NEE phase ($0 < \gamma < 1$), two peaks emerge in the histogram of S : (1) a broad peak whose location roughly scales as N^{-D_1} and (2) a sharp peak at $S = 0$, whose height decreases with N [Fig. 8(a)]. The existence of the second peak [which is absent for RPE, Fig. 8(b), and Heisenberg model, Fig. 8(c)] implies that a small albeit finite fraction of eigenstates are localized for $0 < \gamma < 1$. In Fig. 9(b) we show ξ , the fraction of localized eigenstates as a function of γ for various N . The inset of the same figure shows $\alpha_\xi \approx \gamma - 1$, the system size scaling exponent of ξ , which implies roughly $\xi \propto N^{\gamma-1}$. Thus in the thermodynamic limit, there will be an infinite number of completely localized states in the intermediate regime of β ensemble (since $N^\gamma \rightarrow \infty$ for $\gamma > 0$), which constitutes a zero fraction of all possible eigenstates (since $\xi \rightarrow 0$ for $\gamma < 1$). By looking at the median and mode of IPR of individual eigenstates for

different system sizes, we find that the high-energy states (i.e., the ones in the middle of spectrum) have a greater tendency to be localized compared to the ones close to the ground state in the NEE regime. Thus unlike to RPE, the β ensemble offers two kinds of eigenstates in the NEE phase: N^γ number of completely localized and $(N - N^\gamma)$ number of NEE states.

IV. PROPERTIES OF DYNAMICS

So far we have looked at the statistical picture of the energy level correlation, eigenstate localization, and ergodic properties of the β ensemble. Now we want to look at the dynamical aspects of the β ensemble, revealing important time and energy scales. In this regard, one of the largest timescales is the Heisenberg time, defined as the inverse of mean level spacing. Beyond such a time, the energy level dynamics of a system equilibrates, e.g., the spectral form factor attains a stationary state [84]. Now we explicitly look at the time evolution of an initially localized state and identify the relevant dynamical timescales.

An important characterization of the dynamics of a quantum mechanical system is often done by monitoring the time evolution of a given wave function. We choose a unit vector $|j\rangle$ having energy close to the spectrum center of H as our initial state. Let $(E_k, |\phi_k\rangle)$ be the k th eigenpair of H such that the time evolution of the initial state is given by

$$|j(t)\rangle = e^{-iHt} |j\rangle = \sum_k e^{-iE_k t} \phi_k^{(j)} |\phi_k\rangle, \quad \phi_k^{(j)} = \langle \phi_k | j \rangle. \quad (11)$$

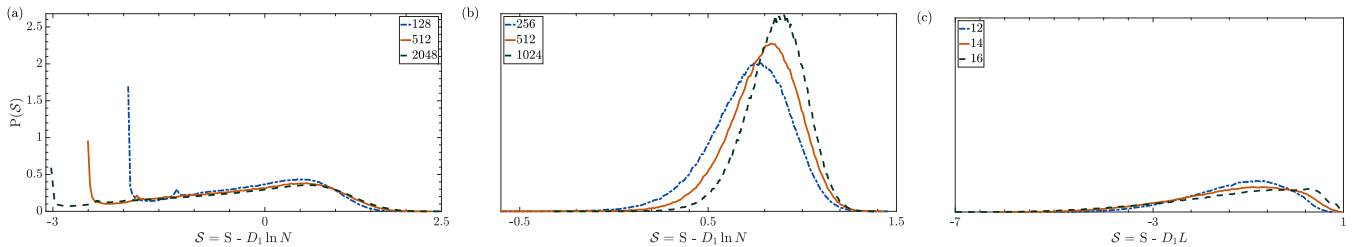


FIG. 8. Density of Shannon entropy: for (a) the β ensemble, $\gamma = 0.6$ (b) RPE, $\tilde{\gamma} = 1.5$, and (c) the Heisenberg model, $h = 2.4$, while varying system sizes, N , and chain lengths, L , where S and S are the scaled and original Shannon entropies, respectively (D_1 is the fractal dimension obtained from system size scaling of S).

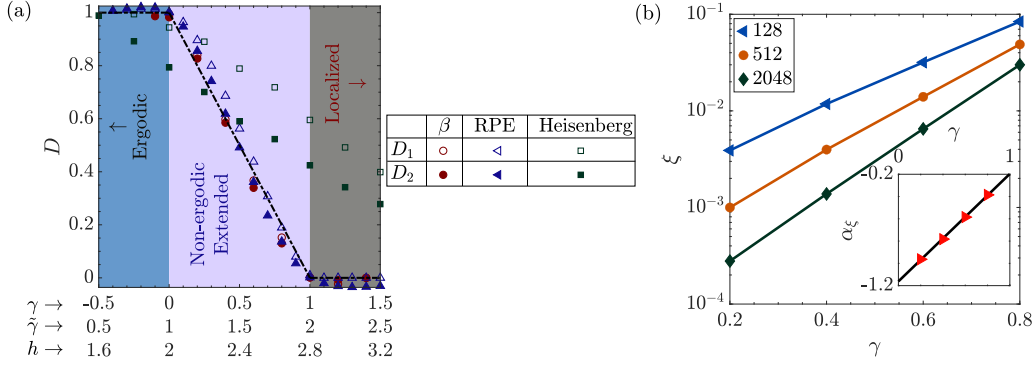


FIG. 9. (a) Phase diagram: The three distinct phases observed in the β ensemble, RPE, and 1D disordered spin-1/2 Heisenberg model are demarcated against the critical parameter values. Markers indicate fractal exponents $D_{1,2}$ as explained in the legend. (b) Fraction of localized states: as a function of γ for the β ensemble for various system sizes. The inset shows α_ξ , the system size scaling exponent of ξ vs γ along with a linear fit, $\alpha_\xi = a\gamma + b$, where $a = 0.9656 \pm 0.0676$ and $b = -1.1618 \pm 0.0370$.

The spread of the initial state $|j\rangle$ over all other states is controlled by the off-diagonal terms in H and is quantified by the survival probability [85]

$$R(t) = |\langle j|j(t)\rangle|^2 = \left| \sum_{k=1}^N |\phi_k^{(j)}|^2 e^{-iE_k t} \right|^2. \quad (12)$$

In general, the survival probability decays till $t = t_{\text{Th}}$, known as the Thouless time [86]. This is the time required for $|j\rangle$ to maximally spread over the Hilbert space. For example, in disordered (ergodic) metals, a particle diffuses to the sample boundaries within t_{Th} . The inverse of t_{Th} gives the Thouless energy, E_{Th} , below which the spectral correlations are similar to those of Wigner-Dyson ensemble. Moreover, a finite-sized closed quantum system always equilibrates [87], and the equilibrium value of survival probability is given by

$$\bar{R} = \lim_{t \rightarrow \infty} \frac{1}{t} \int_0^t d\tau R(\tau) = \sum_{k=1}^N |\phi_k^{(j)}|^4. \quad (13)$$

Thus \bar{R} is the IPR of initial state $|j\rangle$ in the eigenbasis $\{|\phi_k\rangle\}$. The time required to reach \bar{R} is known as the relaxation time, t_{R} . The gap between t_{Th} and t_{R} is known as the correlation hole, t_{hole} . A finite t_{hole} is a direct manifestation of the spectral rigidity, i.e., the presence of long-range correlation among energy levels [54,88,89].

The time evolution of survival probability for β ensemble is shown in Figs. 10(a) and 10(b) for various system sizes and γ values. Tuning γ , we observe three qualitatively different behaviors as follows:

1. *Ergodic regime* ($\gamma \leq 0$). The correlation hole is always present with easily identifiable Thouless and relaxation times. t_{Th} exhibits an approximately \sqrt{N} scaling close to γ_{ET} [inset of Fig. 10(a)], which can be understood from sparsity of the Hamiltonian. Contrarily in the ergodic regime of RPE, t_{Th} is independent of system size due to the presence of all to all coupling [56,90]. We also observe that within t_{hole} , $R(t)$ is nonmonotonic unlike the 1D disordered spin-1/2 Heisenberg model [85].

2. *NEE phase* ($0 < \gamma < 1$). We show t_{hole} as a function of γ for different system sizes in Fig. 10(c) where $t_{\text{hole}} \approx 0$ for $\gamma \geq \gamma^*$. The inset shows that $\gamma^* \rightarrow \gamma_{\text{ET}} = 0$ as N increases.

Recall that the chaotic-integrable transition occurs at γ_{ET} , beyond which long-range correlation among energy levels (e.g., see power spectrum) is lost. The spectral rigidity is necessary for the existence of t_{hole} [88], which explains the absence of the correlation hole in the NEE regime in the thermodynamic limit. On the other hand, a finite t_{hole} exists in the NEE phases of RPE and the 1D disordered spin-1/2 Heisenberg model, as the chaotic-integrable transition occurs at $\tilde{\gamma}_{\text{AT}}$ and h_{MBL} respectively.

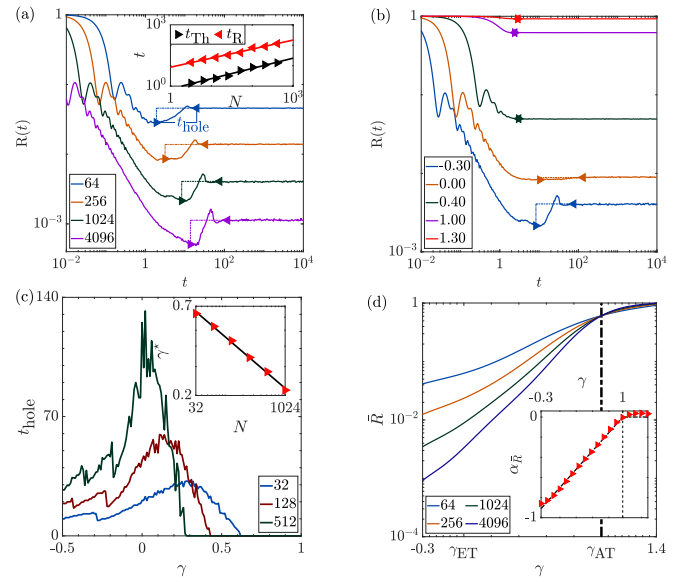


FIG. 10. Survival probability for β ensemble: (a) time evolution for $\gamma = -0.3$ and various system size, N . We show Thouless (t_{Th}) and relaxation time (t_{R}) with markers and the correlation hole (t_{hole}) with a dashed line in each case. The inset shows t_{Th} and t_{R} as a function of N along with linear fit in log-log scale with a solid line, indicating a \sqrt{N} dependence. (b) $N = 1024$ varying γ (c) correlation hole vs γ for various N . The inset shows γ^* vs N in log-log scale ($t_{\text{hole}} \approx 0$ for $\gamma \geq \gamma^*$). (d) Asymptotic value of survival probability vs γ for different N . The inset shows system size scaling ($\bar{R} \propto N^{\alpha_{\bar{R}}}$) where $\alpha_{\bar{R}} \approx \gamma - 1$ for $\gamma \leq 1$ and 0 for $\gamma > 1$.

3. *Localized phase* ($\gamma \geq 1$). Exactly at $\gamma = \gamma_{\text{AT}}$, we observe survival probability curves from different system sizes to collapse on top of each other, showing a critical behavior similar to RPE. In the localized regime (i.e., $\gamma > 1$), t_{hole} is completely absent, while $R(t)$ converges to 1 upon increasing either γ or N .

We show the equilibrium value of survival probability, \bar{R} , as a function of γ in Fig. 10(d). We observe that $\bar{R} \approx 1$ for $\gamma > 1$, which is expected as the initial state, $|j\rangle$, is an eigenstate in the localized regime. The inset of Fig. 10(d) shows system size scaling of \bar{R} , indicating that $\bar{R} \approx N^{\gamma-1}$ in the NEE regime denoting the extent of spread over the Hilbert space for an initially localized state.

V. CONCLUSIONS

In this work we study the spectral properties of β ensemble with a motivation that the competition between diagonal and off-diagonal terms may lead to a NEE phase. As customary in random matrix theory, we discuss the DOS and short-range spectral correlations, namely, NNS and RNNS, and observe a transition from chaos to integrability at $\gamma = 0$. The next pertinent question is whether this transition can be associated with the ergodic and/or localization transitions. A simple analysis of the power spectrum of noise in the eigensequence identifies two critical points: ergodic transition at $\gamma_{\text{ET}} = 0$ and Anderson transition at $\gamma_{\text{AT}} = 1$, separating three distinct phases: the ergodic ($\gamma \leq 0$), NEE ($0 < \gamma < 1$), and localized ($\gamma \geq 1$) phase. Thus similar to RPE [56], related ensembles [91,92] and certain Floquet systems [93–95], the β ensemble is another matrix model where the NEE phase exists over a finite interval of system parameters.

The above observations can be consolidated from the eigenfunction properties as both Shannon entropy and IPR show criticality at $\gamma_{\text{AT}} = 1$, confirming it to be the Anderson transition point. The system size scaling of the above quantities gives us the fractal dimensions $D_{1,2} \approx 1 - \gamma$, clearly demarcating the three phases. For relative Rényi entropies of type 1 and 2, criticality is seen at $\gamma_{\text{ET}} = 0$, thus confirming it to be the chaotic-integrable as well as the ergodic transition point. Moreover, the distribution of Shannon entropy indicates that in the NEE phase, there is a coexistence of N^γ number of a completely localized and $(N - N^\gamma)$ number of NEE states.

Finally, we identify the relevant dynamical timescales from the time evolution of the survival probability, $R(t)$ of an initially localized state and find that the correlation hole, t_{hole} , is always present in the ergodic regime and absent in the NEE phase for $N \gg 1$ as energy levels become uncorrelated. Moreover $R(t) \rightarrow 1$ for $N \gg 1$ and $\gamma > \gamma_{\text{AT}}$ as expected in a localized phase. The NEE phase in the β ensemble is quite distinct from that in RPE, where the energy levels repel each other since integrability breaks down at the Anderson transition point. Again the chaotic-integrable transition point is

energy density dependent, and ergodicity breaks at a lower disorder strength in the case of the 1D disordered spin-1/2 Heisenberg model. We calculate the entropic localization length to explain why chaotic-integrable transition in the β ensemble does not coincide with the localization transition point. These subtle differences imply that the β ensemble is not a suitable model for spin systems like the 1D disordered spin-1/2 Heisenberg model. The proposition that the β ensemble can model Heisenberg chain [62] has also been contradicted in [96,97] via analyses of higher order level spacings and spectral form factor (SFF) and in [65] by studying RNNS crossover. However, in the ergodic regime of the β ensemble, Thouless time scales with the system size similar to sparse Hamiltonians [85]. Thus our analyses suggest that the β ensemble can imitate the spectral properties of various Hamiltonians provided ergodicity breaks down at the chaotic-integrable transition point in such systems.

ACKNOWLEDGMENTS

We thank Lea F. Santos and Ivan Khaymovich for many useful comments on the manuscript. A.K.D. is supported by an INSPIRE Fellowship, DST, India.

APPENDIX: NUMERICAL DETAILS

a. Unfolding. For fixed values of system parameters and size, we obtain $\mathcal{F}(E)$, the cumulative density of eigenvalues from all disordered realizations. Next we smooth $\mathcal{F}(E)$ using a moving average filter. Then for the original eigenvalue E_i , unfolding implies the interpolation of $\mathcal{F}(E_i)$ [10].

b. Scaling of crossover curves. Let us look at an observable y for a system parameter x . If we observe nonanalytical behavior of the corresponding crossover curves from different system sizes, we assume y to behave according to Eq. (7). So we take an array of parameters $\bar{x} = (x(1), x(2), \dots, x(m))$ and measure y for two system sizes N_1 and N_2 , giving us two arrays, $\bar{y}_i = (y_i(1), y_i(2), \dots, y_i(m))$, $i = 1, 2$. Following Eq. (7), we take the function $g(x; x_c, \nu, N) \equiv (x - x_c)(\ln N)^{1/\nu}$. Now we define the function $\bar{x}_i \equiv \bar{x}_i(x_c, \nu) = g(\bar{x}; x_c, \nu, N_i)$ for $i = 1, 2$. For the correct choice of x_c and ν , \bar{y}_1 vs \bar{x}_1 and \bar{y}_2 vs \bar{x}_2 should behave similarly. The observed nonanalyticity of the curves \bar{y}_1 vs γ and \bar{y}_2 vs γ gives a good idea of the initial value of x_c , and we take $\nu = 1$ as the starting value. For these initial choices of x_c and ν , we interpolate \bar{y}_1 vs \bar{x}_1 w.r.t. \bar{x}_2 to create a new array \bar{y}_1 . Next we calculate the residual sum of squares (RSS) between \bar{y}_1 and \bar{y}_2 , defined as $\sum_k (y_1'(k) - y_2(k))^2$. Since RSS should be 0 for the correct choice of x_c and ν , we iteratively change x_c and ν to minimize the RSS, which gives us the desired values of x_c and ν for N_1 and N_2 . We repeat this exercise for all pairs of system sizes and report the average of the obtained parameters.

[1] F. J. Dyson, The threefold way. Algebraic structure of symmetry groups and ensembles in quantum mechanics, *J. Math. Phys.* **3**, 1199 (1962).

[2] A. Altland and M. R. Zirnbauer, Nonstandard symmetry classes in mesoscopic normal-superconducting hybrid structures, *Phys. Rev. B* **55**, 1142 (1997).

- [3] D. A. Ivanov, *Random-Matrix Ensembles in p -Wave Vortices* (Springer, Berlin, 2002), pp. 253–265.
- [4] A. Dubbs, A. Edelman, P. Koev, and P. Venkataramana, The beta-Wishart ensemble, *J. Math. Phys.* **54**, 083507 (2013).
- [5] A. Dubbs and A. Edelman, The beta-Manova ensemble with general covariance, *Random Matrices: Theory Appl.* **03**, 1450002 (2014).
- [6] R. Killip and I. Nenciu, Matrix models for circular ensembles, *Int. Math. Res. Notices* **2004**, 2665 (2004).
- [7] M. L. Mehta, *Random Matrices*, 3rd ed. (Elsevier Science, Amsterdam, 2004).
- [8] F. Borgonovi, F. Izrailev, L. Santos, and V. Zelevinsky, Quantum chaos and thermalization in isolated systems of interacting particles, *Phys. Rep.* **626**, 1 (2016).
- [9] O. Bohigas, M. J. Giannoni, and C. Schmit, Characterization of Chaotic Quantum Spectra and Universality of Level Fluctuation Laws, *Phys. Rev. Lett.* **52**, 1 (1984).
- [10] T. Guhr, A. Müller-Groeling, and H. A. Weidenmüller, Random-matrix theories in quantum physics: Common concepts, *Phys. Rep.* **299**, 189 (1998).
- [11] E. A. Yuzbashyan, B. L. Altshuler, and B. S. Shastry, The origin of degeneracies and crossings in the 1d Hubbard model, *J. Phys. A: Math. Gen.* **35**, 7525 (2002).
- [12] E. Corrigan and R. Sasaki, Quantum versus classical integrability in Calogero–Moser systems, *J. Phys. A: Math. Gen.* **35**, 7017 (2002).
- [13] M. Berry and M. Tabor, Level clustering in the regular spectrum, *Proc. R. Soc. London A* **356**, 375 (1977).
- [14] F. Haake, M. Kuś, and R. Scharf, Classical and quantum chaos for a kicked top, *Z. Phys. B* **65**, 381 (1987).
- [15] A. Y. Abul-Magd, B. Dietz, T. Friedrich, and A. Richter, Spectral fluctuations of billiards with mixed dynamics: From time series to superstatistics, *Phys. Rev. E* **77**, 046202 (2008).
- [16] S. N. Evangelou and J.-L. Pichard, Critical Quantum Chaos and the One-Dimensional Harper Model, *Phys. Rev. Lett.* **84**, 1643 (2000).
- [17] B. I. Shklovskii, B. Shapiro, B. R. Sears, P. Lambrianides, and H. B. Shore, Statistics of spectra of disordered systems near the metal-insulator transition, *Phys. Rev. B* **47**, 11487 (1993).
- [18] T. Brody, A statistical measure for the repulsion of energy levels, *Lett. Nuovo Cimento* **7**, 482 (1973).
- [19] M. V. Berry and M. Robnik, Semiclassical level spacings when regular and chaotic orbits coexist, *J. Phys. A: Math. Gen.* **17**, 2413 (1984).
- [20] F. Izrailev, Quantum localization and statistics of quasienergy spectrum in a classically chaotic system, *Phys. Lett. A* **134**, 13 (1988).
- [21] N. Rosenzweig and C. E. Porter, Repulsion of energy levels in complex atomic spectra, *Phys. Rev.* **120**, 1698 (1960).
- [22] J. X. de Carvalho, M. S. Hussein, M. P. Pato, and A. J. Sargeant, Symmetry-breaking study with deformed ensembles, *Phys. Rev. E* **76**, 066212 (2007).
- [23] G. Casati, L. Molinari, and F. Izrailev, Scaling Properties of Band Random Matrices, *Phys. Rev. Lett.* **64**, 1851 (1990).
- [24] A. D. Mirlin, Y. V. Fyodorov, F.-M. Dittes, J. Quezada, and T. H. Seligman, Transition from localized to extended eigenstates in the ensemble of power-law random banded matrices, *Phys. Rev. E* **54**, 3221 (1996).
- [25] F. Toscano, R. O. Vallejos, and C. Tsallis, Random matrix ensembles from nonextensive entropy, *Phys. Rev. E* **69**, 066131 (2004).
- [26] A. Y. Abul-Magd, Random matrix theory within superstatistics, *Phys. Rev. E* **72**, 066114 (2005).
- [27] C. M. Canali, Model for a random-matrix description of the energy-level statistics of disordered systems at the Anderson transition, *Phys. Rev. B* **53**, 3713 (1996).
- [28] A. Pandey and M. L. Mehta, Gaussian ensembles of random Hermitian matrices intermediate between orthogonal and unitary ones, *Commun. Math. Phys.* **87**, 449 (1983).
- [29] P. Bántay and G. Zala, Ultrametric matrices and representation theory, *J. Phys. A: Math. Gen.* **30**, 6811 (1997).
- [30] F. J. Dyson, Statistical theory of the energy levels of complex systems. I, *J. Math. Phys.* **3**, 140 (1962).
- [31] P. J. Forrester, *Log-Gases and Random Matrices*, London Mathematical Society Monographs Vol. 34 (Princeton University Press, Princeton, 2010).
- [32] T. H. Baker and P. J. Forrester, The Calogero-Sutherland model and generalized classical polynomials, *Commun. Math. Phys.* **188**, 175 (1997).
- [33] P. Choquard, Coulomb system equivalent to the energy spectrum of the Calogero-Sutherland-Moser (CSM) model, *J. Stat. Phys.* **89**, 61 (1997).
- [34] G. Livan, M. Novaes, and P. Vivo, *Classified Material* (Springer International Publishing, Cham, 2018), pp. 53–56.
- [35] G. Le Caër, C. Male, and R. Delannay, Nearest-neighbour spacing distributions of the β -Hermite ensemble of random matrices, *Physica A* **383**, 190 (2007).
- [36] I. Dumitriu and A. Edelman, Matrix models for beta ensembles, *J. Math. Phys.* **43**, 5830 (2002).
- [37] A. Pandey, Statistical properties of many-particle spectra: III. Ergodic behavior in random-matrix ensembles, *Ann. Phys.* **119**, 170 (1979).
- [38] I. Dumitriu, A. Edelman, and G. Shuman, Mops: Multivariate orthogonal polynomials (symbolically), *J. Symbolic Comput.* **42**, 587 (2007).
- [39] J. T. Albrecht, C. P. Chan, and A. Edelman, Sturm sequences and random eigenvalue distributions, *Found. Comput. Math.* **9**, 461 (2009).
- [40] K. Johansson, On fluctuations of eigenvalues of random Hermitian matrices, *Duke Math. J.* **91**, 151 (1998).
- [41] P. Desrosiers and P. J. Forrester, Hermite and Laguerre β -ensembles: Asymptotic corrections to the eigenvalue density, *Nucl. Phys. B* **743**, 307 (2006).
- [42] R. Killip and M. Stoiciu, Eigenvalue statistics for CMV matrices: From Poisson to clock via random matrix ensembles, *Duke Math. J.* **146**, 361 (2009).
- [43] P. Forrester, Global fluctuation formulas and universal correlations for random matrices and log-gas systems at infinite density, *Nucl. Phys. B* **435**, 421 (1995).
- [44] A. Boutet de Monvel, L. Pastur, and M. Shcherbina, On the statistical mechanics approach in the random matrix theory: Integrated density of states, *J. Stat. Phys.* **79**, 585 (1995).
- [45] B. Valkó and B. Virág, Continuum limits of random matrices and the Brownian carousel, *Inventiones mathematicae* **177**, 463 (2009).
- [46] A. Edelman and B. D. Sutton, From random matrices to stochastic operators, *J. Stat. Phys.* **127**, 1121 (2007).

- [47] J. Ramírez, B. Rider, and B. Virág, Beta ensembles, stochastic airy spectrum, and a diffusion, *J. Amer. Math. Soc.* **24**, 919 (2011).
- [48] L. Dumaz and B. Virág, The right tail exponent of the Tracy–Widom β distribution, *Ann. Inst. Henri Poincaré Probab. Stat.* **49**, 915 (2013).
- [49] G. Borot, B. Eynard, S. N. Majumdar, and C. Nadal, Large deviations of the maximal eigenvalue of random matrices, *J. Stat. Mech.: Theory Exp.* (2011) P11024.
- [50] R. Allez and L. Dumaz, Tracy–Widom at high temperature, *J. Stat. Phys.* **156**, 1146 (2014).
- [51] A. Edelman, P.-O. Persson, and B. D. Sutton, Low-temperature random matrix theory at the soft edge, *J. Math. Phys.* **55**, 063302 (2014).
- [52] A. Kumar Das and A. Ghosh, Eigenvalue statistics for generalized symmetric and Hermitian matrices, *J. Phys. A: Math. Theor.* **52**, 395001 (2019).
- [53] L. F. Santos, Integrability of a disordered Heisenberg spin-1/2 chain, *J. Phys. A: Math. Gen.* **37**, 4723 (2004).
- [54] E. J. Torres-Herrera and L. F. Santos, Extended nonergodic states in disordered many-body quantum systems, *Ann. Phys.* **529**, 1600284 (2017).
- [55] D. J. Luitz, N. Laflorencie, and F. Alet, Many-body localization edge in the random-field Heisenberg chain, *Phys. Rev. B* **91**, 081103(R) (2015).
- [56] V. E. Kravtsov, I. M. Khaymovich, E. Cuevas, and M. Amini, A random matrix model with localization and ergodic transitions, *New J. Phys.* **17**, 122002 (2015).
- [57] J. Schenker, Eigenvector localization for random band matrices with power law band width, *Commun. Math. Phys.* **290**, 1065 (2009).
- [58] I. Dumitriu and A. Edelman, Global spectrum fluctuations for the β -Hermite and β -Laguerre ensembles via matrix models, *J. Math. Phys.* **47**, 063302 (2006).
- [59] J. Gustavsson, Gaussian fluctuations of eigenvalues in the GUE, *Ann. Henri Poincaré Probab. Stat.* **41**, 151 (2005).
- [60] T. A. Brody, J. Flores, J. B. French, P. A. Mello, A. Pandey, and S. S. M. Wong, Random-matrix physics: Spectrum and strength fluctuations, *Rev. Mod. Phys.* **53**, 385 (1981).
- [61] M. Pino, J. Tabanera, and P. Serna, From ergodic to non-ergodic chaos in Rosenzweig–Porter model, *J. Phys. A: Math. Theor.* **52**, 475101 (2019).
- [62] W. Buijsman, V. Cheianov, and V. Gritsev, Random Matrix Ensemble for the Level Statistics of Many-Body Localization, *Phys. Rev. Lett.* **122**, 180601 (2019).
- [63] Y. Y. Atas, E. Bogomolny, O. Giraud, and G. Roux, Distribution of the Ratio of Consecutive Level Spacings in Random Matrix Ensembles, *Phys. Rev. Lett.* **110**, 084101 (2013).
- [64] V. Oganessian and D. A. Huse, Localization of interacting fermions at high temperature, *Phys. Rev. B* **75**, 155111 (2007).
- [65] A. L. Corps and A. Relaño, Distribution of the ratio of consecutive level spacings for different symmetries and degrees of chaos, *Phys. Rev. E* **101**, 022222 (2020).
- [66] W. Tang and I. M. Khaymovich, Non-ergodic delocalized phase with Poisson level statistics (2021), [arXiv:2112.09700](https://arxiv.org/abs/2112.09700).
- [67] T. Mondal, S. Sadhukhan, and P. Shukla, Extended states with poisson spectral statistics, *Phys. Rev. E* **95**, 062102 (2017).
- [68] T. Mondal and P. Shukla, Statistical analysis of chiral structured ensembles: Role of matrix constraints, *Phys. Rev. E* **99**, 022124 (2019).
- [69] E. Faleiro, J. M. G. Gómez, R. A. Molina, L. Muñoz, A. Relaño, and J. Retamosa, Theoretical Derivation of $1/f$ Noise in Quantum Chaos, *Phys. Rev. Lett.* **93**, 244101 (2004).
- [70] R. Riser, V. A. Osipov, and E. Kanzieper, Power Spectrum of Long Eigenlevel Sequences in Quantum Chaotic Systems, *Phys. Rev. Lett.* **118**, 204101 (2017).
- [71] A. L. Corps, R. A. Molina, and A. Relaño, Thouless energy challenges thermalization on the ergodic side of the many-body localization transition, *Phys. Rev. B* **102**, 014201 (2020).
- [72] A. L. Corps and A. Relaño, Long-range level correlations in quantum systems with finite Hilbert space dimension, *Phys. Rev. E* **103**, 012208 (2021).
- [73] A. Relaño, L. Muñoz, J. Retamosa, E. Faleiro, and R. A. Molina, Power-spectrum characterization of the continuous Gaussian ensemble, *Phys. Rev. E* **77**, 031103 (2008).
- [74] J. M. G. Gómez, A. Relaño, J. Retamosa, E. Faleiro, L. Salasnich, M. Vraničar, and M. Robnik, $1/f^\alpha$ Noise in Spectral Fluctuations of Quantum Systems, *Phys. Rev. Lett.* **94**, 084101 (2005).
- [75] M. S. Santhanam and J. N. Bandyopadhyay, Spectral Fluctuations and $1/f$ Noise in the Order-Chaos Transition Regime, *Phys. Rev. Lett.* **95**, 114101 (2005).
- [76] Á. Nagy and E. Romera, Relative Rényi entropy and fidelity susceptibility, *Europhys. Lett.* **109**, 60002 (2015).
- [77] S. Sorathia, F. M. Izrailev, V. G. Zelevinsky, and G. L. Celardo, From closed to open one-dimensional Anderson model: Transport versus spectral statistics, *Phys. Rev. E* **86**, 011142 (2012).
- [78] F. M. Izrailev, Simple models of quantum chaos: Spectrum and eigenfunctions, *Phys. Rep.* **196**, 299 (1990).
- [79] G. Casati, B. V. Chirikov, I. Guarneri, and F. M. Izrailev, Band-random-matrix model for quantum localization in conservative systems, *Phys. Rev. E* **48**, R1613 (1993).
- [80] J. Flores, L. Gutiérrez, R. A. Méndez-Sánchez, G. Monsivais, P. Mora, and A. Morales, Anderson localization in finite disordered vibrating rods, *Europhys. Lett.* **101**, 67002 (2013).
- [81] E. Benito-Matías and R. A. Molina, Localization length versus level repulsion in one-dimensional driven disordered quantum wires, *Phys. Rev. B* **96**, 174202 (2017).
- [82] Y. Y. Atas and E. Bogomolny, Multifractality of eigenfunctions in spin chains, *Phys. Rev. E* **86**, 021104 (2012).
- [83] A. D. Mirlin and F. Evers, Multifractality and critical fluctuations at the Anderson transition, *Phys. Rev. B* **62**, 7920 (2000).
- [84] J. Šuntajs, J. Bonča, T. Prosen, and L. Vidmar, Quantum chaos challenges many-body localization, *Phys. Rev. E* **102**, 062144 (2020).
- [85] M. Schiulaz, E. J. Torres-Herrera, and L. F. Santos, Thouless and relaxation time scales in many-body quantum systems, *Phys. Rev. B* **99**, 174313 (2019).
- [86] D. Thouless, Electrons in disordered systems and the theory of localization, *Phys. Rep.* **13**, 93 (1974).
- [87] A. J. Short, Equilibration of quantum systems and subsystems, *New J. Phys.* **13**, 053009 (2011).
- [88] E. J. Torres-Herrera and L. F. Santos, Dynamical manifestations of quantum chaos: Correlation hole and bulge, *Phil. Trans. R. Soc. A* **375**, 20160434 (2017).
- [89] T. Nosaka, D. Rosa, and J. Yoon, The Thouless time for mass-deformed SYK, *J. High Energy Phys.* **01** (2018) 001.

- [90] G. De Tomasi, M. Amini, S. Bera, I. M. Khaymovich, and V. E. Kravtsov, Survival probability in generalized Rosenzweig-Porter random matrix ensemble, *SciPost Phys.* **6**, 014 (2019).
- [91] G. Biroli and M. Tàrzia, Lévy-Rosenzweig-Porter random matrix ensemble, *Phys. Rev. B* **103**, 104205 (2021).
- [92] I. M. Khaymovich, V. E. Kravtsov, B. L. Altshuler, and L. B. Ioffe, Fragile extended phases in the log-normal Rosenzweig-Porter model, *Phys. Rev. Research* **2**, 043346 (2020).
- [93] S. Ray, A. Ghosh, and S. Sinha, Drive-induced delocalization in the Aubry-André model, *Phys. Rev. E* **97**, 010101(R) (2018).
- [94] S. Roy, I. M. Khaymovich, A. Das, and R. Moessner, Multifractality without fine-tuning in a Floquet quasiperiodic chain, *SciPost Phys.* **4**, 025 (2018).
- [95] M. Sarkar, R. Ghosh, A. Sen, and K. Sengupta, Mobility edge and multifractality in a periodically driven Aubry-André model, *Phys. Rev. B* **103**, 184309 (2021).
- [96] P. Sierant and J. Zakrzewski, Model of level statistics for disordered interacting quantum many-body systems, *Phys. Rev. B* **101**, 104201 (2020).
- [97] P. Sierant and J. Zakrzewski, Level statistics across the many-body localization transition, *Phys. Rev. B* **99**, 104205 (2019).